

# Absence of the non-percolating phase for percolation on the non-planar Hanoi network

Takehisa Hasegawa\*

Graduate School of Information Sciences, Tohoku University,  
6-3-09, Aramaki-Aza-Aoba, Sendai, 980-8579, Japan

Tomoaki Nogawa

Department of Mathematics, Tohoku University, 6-3-09,  
Aramaki-Aza-Aoba, Sendai, Miyagi 980-8579, Japan

(Dated: September 10, 2018)

We investigate bond percolation on the non-planar Hanoi network (HN-NP), which was studied in [Boettcher *et al.* Phys. Rev. E 80 (2009) 041115]. We calculate the fractal exponent of a subgraph of the HN-NP, which gives a lower bound for the fractal exponent of the original graph. This lower bound leads to the conclusion that the original system does not have a non-percolating phase, where only finite size clusters exist, for  $p > 0$ , or equivalently, that the system exhibits either the critical phase, where infinitely many infinite clusters exist, or the percolating phase, where a unique giant component exists. Monte Carlo simulations support our conjecture.

PACS numbers: 89.75.Hc 64.60.aq 89.65.-s

## I. INTRODUCTION

Percolation is the simplest model exhibiting a phase transition [1]. Many results for percolation on Euclidean lattices have been reported. It is well known that bond percolation with open bond probability  $p$  on the  $d(\geq 2)$ -dimensional Euclidean lattice shows a second order transition between the non-percolating phase, where only finite size clusters exist, and the percolating phase, where a unique giant component almost surely exists, at a unique critical point  $p_c$ . However, this may not be the case for non-Euclidean lattices.

Complex networks have been actively studied in recent years [2–4]. Among extensive researches carried out on complex networks, percolation on various networks has played an important role in clarifying the interplay between network topology and critical phenomena [5]. Percolation on uncorrelated networks (represented by the configuration model [6]) is well described by the local tree approximation; there is a phase transition between the non-percolating phase and the percolating phase just as in Euclidean lattice systems, but its critical exponents depend crucially on the heterogeneity of the degree distribution of the network [7]. On the other hand, several authors [8–11] have reported that percolation on networks constructed with certain growth rules exhibits quite a different phase transition from that of uncorrelated networks and Euclidean lattices, referred to as an infinite order transition with inverted Berezinskii–Kosterlitz–Thouless (BKT) singularity [12]: (i) The singularity of the phase transition is infinitely weak. When  $p$  lies above the transition point  $p_c$ , the order parameter  $m(p) \equiv \lim_{N \rightarrow \infty} s_{\max}(N; p)/N$ , where  $s_{\max}(N; p)$  is the mean size of the largest cluster

over percolation trials in the system with  $N$  nodes, obeys  $m(p) \propto \exp[-\text{const.}/(\Delta p)^{\beta'}]$ , where  $\Delta p = p - p_c$ . (ii) Below the transition point, the mean number  $n_s$  of clusters with size  $s$  per node obeys the power law,  $n_s \propto s^{-\tau}$ . Furthermore, recent study [13] shows that a hierarchical small-world network exhibits a discontinuous transition instead of an infinite order transition.

In [11, 14, 15], it has been found that, for the growing network models the region below  $p_c$  corresponds to the critical phase (the intermediate phase), which has been observed in nonamenable graphs (NAGs) [16, 17]. NAGs are defined to be transitive graphs with a positive Cheeger constant. Percolation on NAGs (with one end) exhibits the following three phases depending on the value of  $p$ : the non-percolating phase ( $0 \leq p < p_{c1}$ ), the critical phase ( $p_{c1} < p < p_{c2}$ ), where infinitely many infinite clusters exist, and the percolating phase ( $p_{c2} < p \leq 1$ ). Here, an infinite cluster is defined to be a cluster whose size is of order  $O(N^\alpha)$  ( $0 < \alpha \leq 1$ ). It is called a giant component when  $\alpha = 1$ . In the critical phase, where  $0 < \alpha < 1$ , the system is always in a critical state where  $n_s$  satisfies a power law [18].

All previous studies [8–11, 14, 15, 19] of percolation on growing networks and hierarchical small-world networks indicate  $0 = p_{c1} < p_{c2} < 1$ , except in the following case. Boettcher *et al.* investigated bond percolation on the non-planar Hanoi network (HN-NP) using the renormalization group technique [20]. They concluded that there are two critical probabilities  $p_{c1}$  and  $p_{c2}$  between zero and one:  $0 < p_{c1} < p_{c2} < 1$ .

In this paper, we reconsider this model. We show analytically that the fractal exponent of a subgraph, which is a lower bound for that of the HN-NP, takes a non-zero value at all  $p(\neq 0)$ , indicating that  $p_{c1} = 0$ . This means that the system is either in the critical phase or the percolating phase, not in the non-percolating phase, in contrast to the result of [20]. The Monte Carlo simulations support our analytical prediction.

---

\*Electronic address: hasegawa@m.tohoku.ac.jp

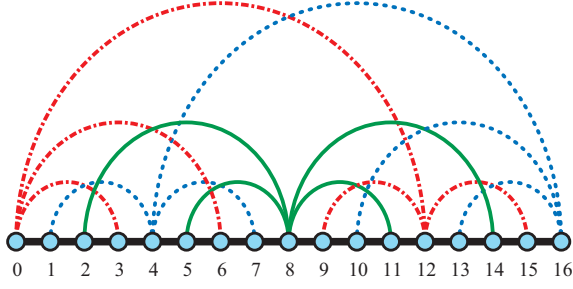


FIG. 1: (Color online) HN-NP with  $L = 4$  generations. The black-thick lines are the backbones, and the red-dashed, green-solid, and blue-dotted lines are the shortcuts of the skeletons  $T_a(4)$ ,  $T_b(4)$ , and  $T_c(4)$ , respectively.

## II. MODEL

The HN-NP consists of a one-dimensional chain and long-range edges. The HN-NP with  $L(\geq 2)$  generation is constructed as follows [20]. (i) Consider a chain of  $N_L = 2^L + 1$  nodes. Here, each node  $i(= 0, 1, 2, \dots, N_L - 1)$  connects to node  $i+1$ . We call these edges the *backbones*. (ii) For each combination of  $i(= 0, 1, 2, \dots, L-2)$  and  $j(= 0, 1, 2, \dots, 2^{L-i-2} - 1)$ , nodes  $(4j+3)2^i$  and  $(4j+4)2^i$  are connected to  $(4j+3)2^i$  and  $(4j+4)2^i$ , respectively. We call these edges the *shortcuts*. The schematic of the HN-NP with  $L = 4$  generations is shown in Fig.1. At generation  $L$ , the number of backbones is  $2^L$  and the number of shortcuts is  $2^L - 2$  (the total number of edges  $E_L$  is  $E_L = 2^{L+1} - 2$ ). The geometrical properties of the HN-NP are as follows [20]: (i) the degree distribution  $p_k$  decays exponentially as  $p_{2m+3} \propto 2^{-m}$ , (ii) the average degree  $\langle k \rangle$  is  $\langle k \rangle = 2E_L/N_L = (2^{L+2}-4)/(2^L+1) \approx 4$  (for  $L \gg 1$ ), (iii) the mean shortest path length  $\langle l \rangle$  increases logarithmically with  $N_L$  as  $\langle l \rangle \propto \log N_L$ , and (iv) the clustering coefficient is zero.

Boettcher *et al.* studied bond percolation on the HN-NP with open bond probability  $p$  [20]. In the HN-NP with  $L$  generations, they considered the renormalization of four parameters:  $R_L$  (the probability that three consecutive points  $a, b, c$  of a chain are connected),  $S_L$  (the probability of  $bc$  being connected, but not  $a$ ),  $U_L$  (the probability of  $ac$  being connected, but not  $b$ ), and  $N'_L$  (the probability that there are no connections among  $a, b$ , and  $c$ ). From the renormalization group flow for  $R_L$  they determined the two critical probabilities as  $p_{c1}^{\text{BCZ}} \approx 0.319445$  and  $p_{c2}^{\text{BCZ}} \approx 0.381966$ .

## III. ANALYTICAL CALCULATION FOR THE SKELETON OF THE HN-NP

The fractal exponent  $\psi_{\max}(p)$  is useful to determine phase behavior [18]. It is defined to be  $\psi_{\max}(p) = \lim_{N_L \rightarrow \infty} \log_{N_L} s_{\max}(N_L; p)$ . A non-percolating phase, a critical phase, and a percolating phase are character-

ized by  $\psi_{\max}(p) = 0$ ,  $0 < \psi_{\max}(p) < 1$ , and  $\psi_{\max}(p) = 1$ , respectively. Unfortunately, it seems difficult to evaluate  $s_{\max}(N_L; p)$  directly for the HN-NP. Instead, we focus on a subgraph of the HN-NP and evaluate its fractal exponent.

We extract a subgraph from the HN-NP with  $L$  generations by removing the backbones. Because the resulting subgraph has no cycles and the number of shortcuts is  $2^L - 2 = N_L - 3$ , this subgraph is composed of three disconnected trees. Indeed, nodes  $i = 0, 2^{L-1}$ , and  $2^L$  belong to the three different trees. We call these *the root nodes*. Here the graphs isomorphic to these trees and having root nodes  $i = 0, 2^{L-1}$ , and  $2^L$  will be called the *skeletons*  $T_a(L)$ ,  $T_b(L)$ , and  $T_c(L)$ , respectively. Clearly,  $T_a(L)$  and  $T_c(L)$  are also isomorphic to each other,  $T_a(L) \simeq T_c(L)$ . At  $L = 2$ ,  $T_a(2)$  is composed of nodes 0 and 3 and the edge between them,  $T_b(2)$  is one isolated node  $i = 2$ , and  $T_c(2)$  is composed of nodes 1 and 4 and the edge between them. The skeletons  $T_a(L)$ ,  $T_b(L)$ , and  $T_c(L)$  for arbitrary  $L$  are given recursively as follows. First, we consider two subgraphs of the sets of nodes  $\{0, 1, \dots, 2^{L-1}\}$  and  $\{2^{L-1}, 2^{L-1}+1, \dots, 2^L\}$  after removing the backbones from the HN-NP with  $L$  generations. By symmetry, both subgraphs consist of the skeletons  $T_a(L-1)$ ,  $T_b(L-1)$ , and  $T_c(L-1)$  (Fig.2(a)). Here the root nodes of the latter subgraph are  $i = 2^{L-1}$  (for  $T_c(L-1)$ ),  $3 \times 2^{L-2}$  (for  $T_b(L-1)$ ), and  $2^L$  (for  $T_a(L-1)$ ). Note that the skeletons  $T_a(L)$ ,  $T_b(L)$ , and  $T_c(L)$  are given by adding the two long-range edges  $\{0, 3 \times 2^{L-2}\}$  and  $\{2^{L-2}, 2^L\}$ , and taking into account the connection of node  $2^{L-1}$  (Fig.2(b)), we have

$$T_a(L) \simeq T_c(L) \simeq R_1(T_a(L-1), T_b(L-1)), \quad (1)$$

$$T_b(L) \simeq R_2(T_c(L-1), T_c(L-1)), \quad (2)$$

where the operation  $R_1(x, y)$  adds the edge between root nodes of the skeletons  $x$  and  $y$ , and  $R_2(x, y)$  merges two root nodes of the skeletons  $x$  and  $y$  into one.

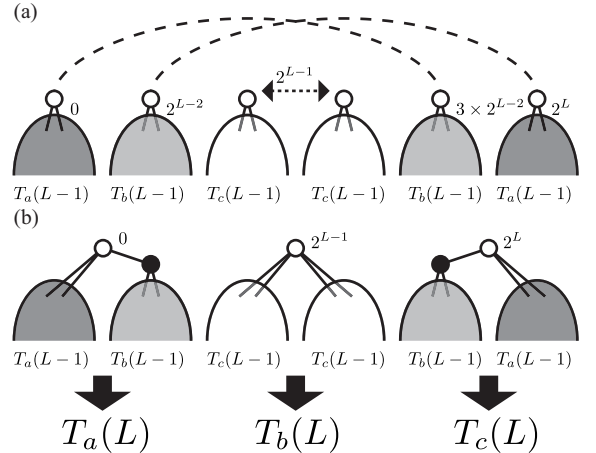


FIG. 2: Construction of the skeletons  $T_a(L)$ ,  $T_b(L)$ , and  $T_c(L)$ . Open circles represent the root nodes of the skeletons.

We now calculate the mean size of a cluster including the root node (the root cluster size) for each skeleton. We denote the root cluster sizes of  $T_a(L)$  ( $\simeq T_c(L)$ ) and  $T_b(L)$  by  $s_a(L)$  and  $s_b(L)$ , respectively. Because of the recursive structure (1, 2) of the skeletons, the root cluster sizes  $s_a(L)$  and  $s_b(L)$  also satisfy recursive relations:

$$s_a(L+1) = s_a(L) + ps_b(L), \quad (3)$$

$$s_b(L+1) = 2s_a(L) - 1, \quad (4)$$

where the initial conditions are  $s_a(2) = 1+p$  and  $s_b(2) = 1$ . Then, we find that

$$s_a(L) = \frac{1}{2} + \frac{(1 + \sqrt{1+8p})^{L+1} - (1 - \sqrt{1+8p})^{L+1}}{2^{L+2}\sqrt{1+8p}} \quad (5)$$

$$s_b(L) = 1 + \frac{(1 + \sqrt{1+8p})^L - (1 - \sqrt{1+8p})^L}{2^L\sqrt{1+8p}}. \quad (6)$$

For  $L \gg 1$ , we obtain  $s_a(L) \propto N_L^{\psi_{\text{root}}^{\text{skeleton}}(p)}$ , where

$$\psi_{\text{root}}^{\text{skeleton}}(p) = \log_2(1 + \sqrt{1+8p}) - 1. \quad (7)$$

We expect  $\psi_{\text{root}}^{\text{skeleton}}(p) = \psi_{\text{max}}^{\text{skeleton}}(p)$  because the roots are hubs. In fact, we performed Monte Carlo simulations for the bond percolation on the skeletons. Our numerical result of  $\psi_{\text{max}}^{\text{skeleton}}(p)$  shows a good correspondence with Eq.(7) except near  $p = 0$  (not shown). According to Eq.(7),  $\psi_{\text{root}}^{\text{skeleton}}(p)$  increases continuously from  $\psi_{\text{root}}^{\text{skeleton}}(0) = 0$  to  $\psi_{\text{root}}^{\text{skeleton}}(1) = 1$ . This means that the subsystem consisting only of the shortcuts is in the critical phase for all  $p (\neq 0, 1)$ , like the growing random tree [15]. Because the HN-NP is obtained by adding the backbones to the skeletons, the clusters in the skeletons become larger. Therefore, the entire system permits a critical phase even for infinitesimal  $p$ , i.e., the non-percolating phase does not exist except at  $p = 0$ .

#### IV. NUMERICAL CHECK

In the previous section, we evaluated the root cluster size of the skeleton to show that its fractal exponent  $\psi_{\text{root}}^{\text{skeleton}}(p)$  takes a non-zero value for all  $p > 0$ . Because the skeleton is just a subgraph of the HN-NP,  $\psi_{\text{root}}^{\text{skeleton}}(p)$  is a lower bound for the fractal exponent of the largest cluster of the HN-NP  $\psi_{\text{max}}^{\text{HN-NP}}(p)$ , i.e.,  $\psi_{\text{root}}^{\text{skeleton}}(p) \approx \psi_{\text{max}}^{\text{HN-NP}}(p) \leq \psi_{\text{max}}^{\text{HN-NP}}(p)$ . For bond percolation on the HN-NP,  $\psi_{\text{max}}^{\text{HN-NP}}(p) > 0$  when  $p > 0$ , implying that  $p_{c1} = 0$ . To check our prediction, we performed Monte Carlo simulations of bond percolation on the HN-NP. The number of generations is  $L = 13, 14, \dots, 20$ , and the number of percolation trials is 100000 for each  $p$ .

Figures 3(a) and (b) show the results for the order parameter  $m(N_L; p)$  and the fractal exponent of the largest cluster  $\psi_{\text{max}}^{\text{HN-NP}}(N_L; p)$ , respectively. Here the fractal exponent  $\psi_{\text{max}}^{\text{HN-NP}}(N_L; p)$  at a finite generation  $L$  is evalu-

ated as

$$\psi_{\text{max}}^{\text{HN-NP}}(N_L; p) \approx \frac{\log s_{\text{max}}(N_{L+1}; p) - \log s_{\text{max}}(N_{L-1}; p)}{\log N_{L+1} - \log N_{L-1}}. \quad (8)$$

We also plot the fractal exponent  $\psi_{\text{root}}^{\text{skeleton}}(p)$  of the skeleton (Eq.(7), shown as the thick-dashed line) and  $p_{c1}^{\text{BCZ}}$  and  $p_{c2}^{\text{BCZ}}$  (shown as vertical lines) in Fig.3.

From Fig.3(b), we see that  $\psi_{\text{root}}^{\text{skeleton}}(p)$  is actually the lower bound of  $\psi_{\text{max}}^{\text{HN-NP}}(p)$ , implying that  $p_{c1} = 0$ . In particular,  $\psi_{\text{max}}^{\text{HN-NP}}(N_L; p)$  coincides with  $\psi_{\text{root}}^{\text{skeleton}}(p)$  for  $p \lesssim 0.26$  (except near  $p = 0$ , where finite size effects are not negligible). For  $p \gtrsim 0.26$ ,  $\psi_{\text{max}}^{\text{HN-NP}}(N_L; p)$  is considerably greater than  $\psi_{\text{root}}^{\text{skeleton}}(p)$ , and reaches unity at  $p = p_{c2}^{\text{BCZ}}$ . At a glance, in the large size limit,  $\psi_{\text{max}}^{\text{HN-NP}}(N_L; p)$  seems to change continuously with  $p < p_{c2}^{\text{BCZ}}$ . However, we speculate that in the large size limit  $\psi_{\text{max}}^{\text{HN-NP}}(N_L; p)$  (i) coincides with  $\psi_{\text{root}}^{\text{skeleton}}(p)$  in the entire region below  $p_{c1}^{\text{BCZ}}$ , (ii) jumps to a higher value at  $p = p_{c1}^{\text{BCZ}}$ , and (iii) increases monotonically up to unity for  $p_{c1}^{\text{BCZ}} < p \leq p_{c2}^{\text{BCZ}}$ . The coincidence between  $\psi_{\text{max}}^{\text{HN-NP}}(p)$  and  $\psi_{\text{root}}^{\text{skeleton}}(p)$  for

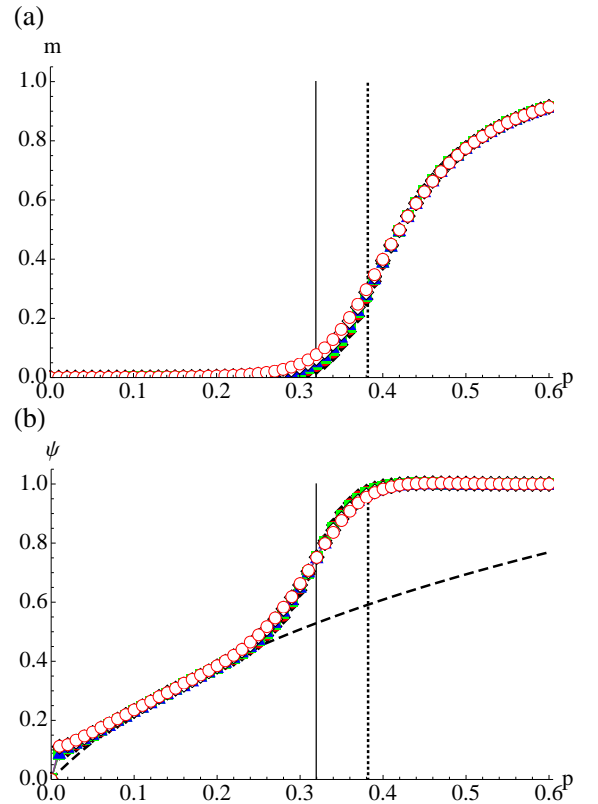


FIG. 3: (Color online) (a) Order parameter  $m(N_L; p) = s_{\text{max}}(N_L; p)/N_L$  and (b) fractal exponent  $\psi(N_L; p)$ . The numbers of generations  $L$  are 19 (black-diamond), 18 (red-circle), 17 (green-square), 16 (blue-triangle), 15 (open-diamond), and 14 (open-circle). The vertical solid line and dashed line indicate  $p_{c1}^{\text{BCZ}}$  and  $p_{c2}^{\text{BCZ}}$  respectively. In (b), the fractal exponent  $\psi_{\text{root}}^{\text{skeleton}}(p)$  of the skeleton given by Eq.(7) is shown by the thick-dashed line.

$p < p_{c1}^{\text{BCZ}}$  means that the partial ordering (in the sense that the largest cluster is  $O(N^\alpha)$  with  $\alpha < 1$ ) in this region is essentially governed by the shortcuts. Because Boettcher *et al.* [20] considered renormalization of the connecting probability of consecutive points of the backbones, we would expect their first critical probability  $p_{c1}^{\text{BCZ}}$  to be the probability above which the backbones become relevant. Thus, we expect that there is a transition between critical phases, in the sense that the fractal exponent jumps, implying a qualitative change in the criticality, while it is very difficult to judge whether such a transition exists or not by finite size simulations. Such a jump in the fractal exponent has already been observed in site-bond percolation on the decorated (2,2)-flower [21]. In addition, our numerical result shows that  $\psi_{\text{max}}^{\text{HN-NP}}(p)$  reaches unity smoothly at  $p_{c2}^{\text{BCZ}}$ . This indicates that the phase transition to the percolating phase is discontinuous, similarly as in [13].

Finally, we discuss the cluster size distribution function,  $n_s(p)$ , below  $p_{c2}^{\text{BCZ}}$ . Figure 4(a) shows  $n_s(p)$  for several values of  $p$  with  $0 < p < p_{c2}^{\text{BCZ}}$ . In the critical

phase, we expect a power law for  $n_s(p)$ :

$$n_s(p) \propto s^{-\tau(p)}, \quad (9)$$

where

$$\tau(p) = 1 + \psi_{\text{max}}(p)^{-1}, \quad (10)$$

and a corresponding scaling form:

$$n_s(N_L; p) = N_L^{-\psi_{\text{max}}(p)\tau(p)} f(sN_L^{-\psi_{\text{max}}(p)}), \quad (11)$$

where the scaling function  $f(\cdot)$  behaves as

$$f(x) \sim \begin{cases} \text{rapidly decaying func.} & \text{for } x \gg 1, \\ x^{-\tau(p)} & \text{for } x \ll 1. \end{cases} \quad (12)$$

We tested this scaling for  $0 < p \lesssim 0.26$  and  $p_{c1}^{\text{BCZ}} < p < p_{c2}^{\text{BCZ}}$  and obtained excellent collapses (Fig.4(b)). We would also expect that  $n_s$  to be fat-tailed for  $0.26 \lesssim p < p_{c1}^{\text{BCZ}}$  because  $n_s(p)$  for the skeletons perfectly obeys Eqs.(9) and (10) via Eq.(11) for  $0 < p < 1$  (not shown), and  $n_s$  is broader when we add the backbones to the skeletons, i.e., for the original HN-NP.

## V. SUMMARY

In this paper, we have studied bond percolation on the HN-NP. Our results give the two critical probabilities as  $p_{c1} = 0 (< p_{c1}^{\text{BCZ}})$  and  $p_{c2} = p_{c2}^{\text{BCZ}}$ , implying that the system has only a critical phase and a percolating phase, and does not have a non-percolating phase for  $p > 0$ . As far as we know, all complex network models with a critical phase have only the critical phase and the percolating phase ([8–11, 13–15, 19] for percolation and [12, 19, 22–27] for spin systems). It will be challenging to clarify the origin of such universal behavior.

## Acknowledgments

TH acknowledges the support through Grant-in-Aid for Young Scientists (B) (No. 24740054) from MEXT, Japan.

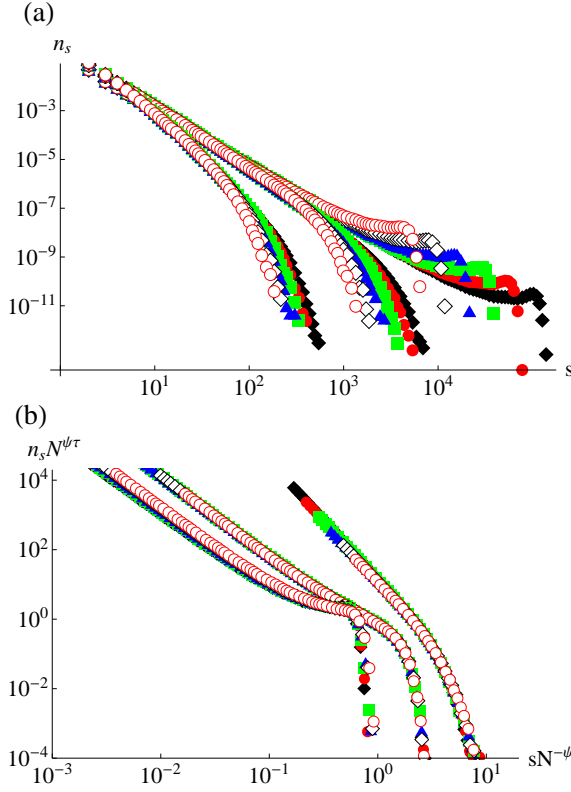


FIG. 4: (Color online) (a) Cluster size distribution  $n_s(N_L; p)$  at  $p = 0.16$ ,  $0.26 (< p_{c1}^{\text{BCZ}})$ , and  $0.36 (> p_{c1}^{\text{BCZ}})$ , from left to right. (b) Scaling result for  $n_s(N_L; p)$  at  $p = 0.20 (< p_{c1}^{\text{BCZ}})$ ,  $0.32$ , and  $0.35 (> p_{c1}^{\text{BCZ}})$ , from right to left. The numbers of generations  $L$  are 19 (black-diamond), 18 (red-circle), 17 (green-square), 16 (blue-triangle), 15 (open-diamond), and 14 (open-circle).

- 
- [1] D. Stauffer and A. Aharony, *Introduction to Percolation Theory* (Taylor and Francis, London, 1994).
  - [2] R. Albert and A.-L. Barabási, *Rev. Mod. Phys.* **74**, 47 (2002).
  - [3] M. E. J. Newman, *SIAM review* **45**, 167 (2003).
  - [4] A. Barrat, M. Barthélemy, and A. Vespignani, *Dynamical processes on complex networks* (Cambridge University Press, Cambridge, 2008).
  - [5] S. N. Dorogovtsev, A. V. Goltsev, and J. F. F. Mendes, *Rev. Mod. Phys.* **80**, 1275 (2008).
  - [6] M. Molloy and B. Reed, *Random Struct. Algor.* **6**, 161 (1995).
  - [7] R. Cohen, D. ben Avraham, and S. Havlin, *Phys. Rev. E* **66**, 036113 (2002).
  - [8] D. S. Callaway, J. E. Hopcroft, J. M. Kleinberg, M. E. J. Newman, and S. H. Strogatz, *Phys. Rev. E* **64**, 041902 (2001).
  - [9] S. N. Dorogovtsev, J. F. F. Mendes, and A. N. Samukhin, *Phys. Rev. E* **64**, 066110 (2001).
  - [10] L. Zálányi, G. Csárdi, T. Kiss, M. Lengyel, R. Warner, J. Tobochnik, and P. Érdi, *Phys. Rev. E* **68**, 066104 (2003).
  - [11] T. Hasegawa, M. Sato, and K. Nemoto, *Phys. Rev. E* **82**, 046101 (2010).
  - [12] M. Hinczewski, and A. N. Berker, *Phys. Rev. E* **73**, 066126 (2006).
  - [13] S. Boettcher, V. Singh, and R. M. Ziff, *Nature Communications* **3**, 787 (2012).
  - [14] T. Hasegawa, T. Nogawa, and K. Nemoto, arXiv: 1009.6009 (2010).
  - [15] T. Hasegawa and K. Nemoto, *Phys. Rev. E* **81**, 051105 (2010).
  - [16] I. Benjamini and O. Schramm, *Electron. Comm. Probab.* **1**, 71 (1996).
  - [17] R. Lyons, *J. Math. Phys.* **41**, 1099 (2000).
  - [18] T. Nogawa and T. Hasegawa, *J. Phys. A: Math. Theor.* **42**, 145001 (2009).
  - [19] A. N. Berker, M. Hinczewski, and R. R. Netz, *Phys. Rev. E* **80**, 041118 (2009).
  - [20] S. Boettcher, J. L. Cook, and R. M. Ziff, *Phys. Rev. E* **80**, 041115 (2009).
  - [21] T. Hasegawa, M. Sato, and K. Nemoto, *Phys. Rev. E* **85**, 017101 (2012).
  - [22] M. Bauer, S. Coulomb, and S. N. Dorogovtsev, *Phys. Rev. Lett.* **94**, 200602 (2005).
  - [23] E. Khajeh, S. N. Dorogovtsev, and J. F. F. Mendes, *Phys. Rev. E* **75**, 041112 (2007).
  - [24] S. Boettcher and C. T. Brunson, *Phys. Rev. E* **83**, 021103 (2011).
  - [25] S. Boettcher and C. Brunson, *Front. Physiol.* **2**, 102 (2011).
  - [26] T. Nogawa, T. Hasegawa, and K. Nemoto, *Phys. Rev. Lett.* **108**, 255703 (2012).
  - [27] T. Nogawa, T. Hasegawa, and K. Nemoto, *Phys. Rev. E* **86**, 030102 (2012).